SCIREA Journal of Materials Science

http://www.scirea.org/journal/Materials

December 27, 2016

# Corrosion behavior of anodized Al coated by Physical vapor deposition method on Cu-10Al-13Mn shape memory alloy

**Hossein Aghajani[1,*], Davoud Pourabbas[1], Mirali Seyed Shariatdoust[1],**

[1]Department of Materials Engineering, Faculty of Mechanical Engineering, University of Tabriz, Tabriz 51666-16471, Iran

* Corresponding author. Tel.: +98 41333354200; fax: +98 41333354153

Email addresses: H_Aghajani@tabrizu.ac.ir (H. Aghajani)

Address: University of Tabriz, Faculty of Mechanical Engineering, Department of Materials Science and Engineering, Tabriz, Iran

## Abstract

Physical vapor deposition method was utilized to apply Al coating onto Cu-10Al-13Mn alloy, then coated layer was anodized in different temperatures: 5˚C and 10˚C as well as several potentials: 20V, 30V, 40V, 50V in order to achieve best anodizing parameters. The effects of anodizing parameters on alumina nanotube formation and corrosion resistance were investigated. Phase analysis on surface was conducted by X-ray diffraction method and nanotube characteristics was studied by scanning electron microscopy (SEM) and surface topology was investigated by atomic force microscopy (AFM). Additionally, the corrosion resistance of coatings was studied by potentiodynamic test in 1M NaCl solution. The results depicted that whole deposited Al layer was anodized and FCC alumina was formed merely. Polarization test results was illustrated that Al anodized layer significantly improved Cu-

10Al-13Mn corrosion resistance. Uncoated specimen had highest corrosion rate and anodized layer in lower temperature and voltage had minimum alumina nanotube dimension; as a result, it had best corrosion behavior in NaCl corrosive solution.

**Keywords:** Cu-10Al-13Mn; shape memory alloy; aluminum anodizing; corrosion

## 1. Introduction

Shape memory alloys are attractive materials in smart mechanical systems, inductors in aerospace industries and medical equipment. NiTi alloys are practical due to their appropriate superelasticity, corrosion and electrical resistance; however, production sensitivity as well as high manufacturing costs make Cu based shape memory alloys serious competitor to NiTi alloys for their formability, machinability and conductivity [1].

Additionally, choosing proper chemical composition in Cu based shape memory alloys can eventuate in having shape memory effect in low temperatures [2]. Adding Mn to Cu-Al system lowers Ms and stabilize β phase [3]. More aluminum and manganese existence in alloy composition cause thicker martensite plates and twining in microstructure which aluminum has more effect [4]. Cu-Al-Mn alloys with lower aluminum and higher manganese have better shape memory effect due to irregularity in their atomic structure [5]. It has been reported that shape memory effect and superelasticity effect in Cu-Al-Mn alloys are 7% and 5%, respectively [6].

Moreover, pure Cu has acceptable resistance to corrosion in clean atmosphere [7]. On the other hand, Cu-Al alloys with aluminum percentage higher than 8% have poor corrosion resistance in chloride solutions due to their dealumination and production of other phases than α [8-11].

Corrosion resistance of materials can be improved by surface modifying by methods like electroplating, chemical vapor deposition, physical vapor deposition and ion implanting. Physical vapor deposition is one of the most practical and green methods of surface coating [12, 13, 14]. Furthermore, Al coating improves corrosion resistance. Anodizing improves corrosion resistance, wear resistance, electricity insulation and further coating adherence [15]. Anodizing parameters such as: substrate, electrolyte, current density, temperature and potential play crucial role in final anodized layer quality [16, 17]. Anodizing process notably increases coated aluminum layer corrosion resistance; therefore, it can give better characteristics to the alloy surface in corrosive media [18-21].

Some previous investigations illustrate that anodized aluminum coating improves corrosion resistance of aluminum alloys (1070, 2024, 7075) in NaCl solution [22], magnesium alloy (AZ31) [23], Al-Si alloy substrates [24].

Given the fact the few studies have been conducted into the effect of anodized aluminum coating on the corrosion resistance of Cu-Al-Mn shape memory alloys. The aim of this study is to apply the Al coating on the Cu-10Al-13Mn alloy by PVD method and anodizing coated layer with various potentials and temperatures then investigate characteristics of formed alumina nanotubes and the corrosion resistance of theses coatings using polarization test.

## 2. Materials and method

In this study Cu-10Al-13Mn with chemical composition in table.1 was utilized as substrate. Cu-10Al-13Mn alloy was produced by melting high purity Cu (99.98%), and adding 20-80 Al-Mn alloy to the melt in 1100˚C. In order to prevent Al oxidation and evaporation, glass was added to the melt surface. Glass was removed from melt surface after melt homogenization. Inclusions were removed from melt by adding NaCl. Melting and solidification process were implemented for more purification and homogenization several times and then ingots were casted. Samples were cut to the size of 10mm ×20mm ×3mm and abraded and polished with 100-1000 emery paper and $Al_2O_3$ paste ($1\mu m$), respectively. Before Al layer deposition, specimens were washed in phosphoric acid and deionized water; then, placed in nitric acid and chloridric acid solutions, respectively and then washed in distilled water. Oxide layer was removed with 200 emery paper. Al layer was coated on specimens by physical vapor deposition method. Coating duration was 3hr and final Al layer thickness was $27\mu m$ and coating chamber pressure was $10^{-5} torr$ during the process. After Al coating process all specimens were degreased in $NaOH\left(100\ {}^{gr}/_{l}\right)$, and $Na_2CO_3\left(40\ {}^{gr}/_{l}\right)$ solution. Afterward, specimens placed in HCl (10%wt) solution in order to eliminate any remained oxides on the surface.

Anodizing process was performed in standard $H_2C_2O_4$ solution ($0.3{}^{mol}/_{l}$). Anodizing was implemented using following different potentials: 20V, 30V, 40V and 50V as well as different temperatures: 5˚C and 10˚C. In table.2 specimens are defined by anodizing temperature and potential, in which first two digits depict anodizing temperature and second two digits illustrate anodizing potential. Moreover, in order to attain uniform anodized Al surface, anodizing bath temperature and composition were controlled by Benmari bath and

mechanical mixer. Anode and Cathode distance was 50 mm and anodizing process duration was 60 min for all specimens.

Phase analysis of surface was defined by X-ray diffraction (Bruker AXS, Advance D8). Additionally, surface was investigated by scanning electron microscopy (SEM, ROVENTEC vega II XMU/TESCAN); furthermore, surface topography, morphology and roughness was studied by atomic force microscopy (AFM, Nanoscope ® III).

Finally, corrosion behavior of anodized Al layer on Cu-10Al-13Mn was investigated by potentiodynamic polarization test using an Autolab potentiostat/galvanostat (EG & G, PARSTAT 2263) in 1M NaCl solution at open circuit potential. The Cu-10Al-13Mn alloy sample was the working electrode in test set-up. In addition, a platinum mesh and a saturated calomel electrode (SCE) were utilized as the auxiliary electrode and the reference electrode in the cell, respectively. Potentiodynamic polarization tests were performed at potential sweeping rate of 2mV/s in 1M NaCl solution. These tests were carried out to investigate the electrochemical behaviors of Cu-10Al-13Mn alloy in Chloride solution.

## 3. Results and discussion

### 3.1 Al Coating

Fig.1 shows surface and cross section of Al coating on Cu-10Al-13Mn after coating process. As seen from Fig.1 (a) there are domical cavities on the surface which are resulted from substrate's surface deficiencies. These defects absorb Al atoms during deposition due to their lower surface energy for aluminum nucleation on substrates surface; moreover, there is no crack on surface after deposition process. Fig. 1 (b) shows the thickness of deposited Al layer which is approximately 27 μm.

Phase and elemental analysis by X-ray diffraction also substantiates Al coating formation. As seen from Fig. 2. There is no other phase than Al formed in coating layer on the Cu-10Al-13Mn substrate in all samples.

### 3.2 Anodizing

Although surface color change while anodizing can be encountered as alumina formation; however, aluminum transformation to the alumina makes meaningful difference to current density of anodic oxidation. Fig. 3 depicts current density change by time which it has same trend for all specimens. As seen from Fig. 3, first current density shows notable drop for oxide formation on the coated layer; as the anodizing process progresses, the hole layer is anodized and then anodized layer begin to be dissolving and current density increasing. Also

in Fig. 4 X-ray diffraction patterns after anodizing process confirm aluminum oxide formation on the surface.

### 3.3 Alumina nanotubes Dimensions

Alumina-tubes dimensions are measured by tubes diameter and height in general. Since whole Al layer has been anodized; therefore, tubes height are similar to the coated layer thickness. For investigation of different anodizing parameters on alumina-tubes inner and outer diameters on specimen surface, scanning electron microscope (SEM) was utilized. Fig. 5 depicts some of the SEM micrographs. Also, average of diameter dimension is reported for both inner and outer tubes, respectively. As it can be seen from results, tubes are in nanometric scale. Additionally, both dimensions of inner and outer diameter change by temperature and potential are shown in fig. 6.

According to Fig. 6 alumina nanotube diameters increase with temperature acceleration in constant potential. As seen from eq.1 temperature increase, eventuates in anodic yield decrease which also results in nanotubes nucleation locations drop; as a result; nanotube size increases.

$$2Al_{(s)} + 3[O] = Al_2O_{3_{(s)}} \quad \text{(eq.1)}$$

In either plating or electrolyze processes in aqueous solution maximum hydrogen voltage decreases with temperatures increase in constant current density which it produces more hydrogen gas in high temperatures. It wanes $H^+$ in cathode layer and low pH in cathode layer prevents $H^+$ reduction; therefore; layer stress declines and external diameter increases. Fig. 6 shows nanotubes diameter augmentation with voltage increase. In regard to eq.1, current density increase causes cathode yield augmentation in constant plating temperature. Inner and outer nanotube diameters obey same pattern in anodizing process conditions.

### 3.4 Surface Roughness

In addition, surface morphology was investigated by atomic force microscopy (AFM) in order to roughness evaluation. Four specimens of reference, Al coated, A0520 (specimen with lowest anodizing temperature and potential) and A1050 (specimen with highest anodizing temperature and potential) were conducted into surface morphology and roughness. As seen from Fig. 7 general roughness increases by anodizing process and coating of aluminum on the substrate resulted in four times rougher surface which is related to domical cavities in the surface; however; by using anodizing process, surface reaches eight times rougher surface than uncoated specimen. Roughness differs in range of 40 nm for A0520 to 70 nm for A1050. Fig. 7 depicts that anodized specimen in low voltage and temperature has less roughness than

specimen anodized in higher voltage and temperature. It can be noticed that surface roughness has direct relation with dimension of alumina nanotubes diameter and anodized surface roughness so it can be controlled by anodizing parameters changes.

## 4. Potentiodynamic Tests

Fig. 8 illustrates polarization curves that were obtained from specimens: uncoated, Al coated, A0520, A1050. Polarization resistance can be calculated by polarization test results and eq.2:

$$R_P = \frac{\beta_a \times \beta_c}{2.303 \times i_{corr} \times (\beta_a + \beta_c)} \quad \text{(eq.2)}$$

In eq.2, $\beta_a$ and $\beta_c$ are tafel curve slopes and $i_{corr}$ is corrosion current; also, corrosion rate calculated using eq.3:

$$mpy = \frac{345 \times M \times i_{corr}}{Z \times D \times F} \quad \text{(eq.3)}$$

M is base metal atomic mass ($65^{gr}/_{mol}$), D is density ($8.35^{gr}/_{cm^3}$), F is Faraday's number and Z is defined as atomic capacity.

Table 3 is derived from eq.2, eq.3, and polarization curves and it shows that uncoated specimen due to its high corrosion current has minimum corrosion resistance; also, polarization curves illustrate that there are no passive behavior in 3.5(wt%)NaCl solution in none of the specimens. According to table 3, uncoated specimen has higher corrosion potential than other specimens (-0.34V), it has maximum corrosion rate. In addition, specimens with lower anodizing potential and temperature have lower corrosion rate; similarly, specimens with higher anodizing potential and temperature have higher polarization resistance as well. As it can be seen from table 3, all anodized specimens have lower corrosion rate than either uncoated or Al coated specimens. In comparison to other anodized specimens it can be noticed that high potential and temperature anodizing condition which has been produced high surface nanotube inner diameter, has lower corrosion resistance; furthermore; the nanotubes can lead corrosive solution to the substrate and exacerbate corrosion.

## 5. Conclusion

It can be concluded that using different potentials: 5 ˚C, 10 ˚C, and different temperatures: 20 V, 30 V, 40 V and 50V eventuated in anodizing whole physical vapor deposited aluminum layer (27 µm) on Cu-10Al-13Mn shape memory alloy. Also, XRD analysis substantiated

alumina formation on coated aluminum layer after anodizing process. Furthermore, SEM micrographs depicted that inner and outer diameter of alumina nanotubes increased by voltage and temperature increasing during anodizing process. It was observed that highest corrosion rate related to uncoated specimen and the best corrosion resistance is related to lowest anodizing temperature and potential, respectively, according to polarization tests results; as a result, best results toward highest corrosion resistance achieved in condition of anodizing potential and temperature 5V and 20 ˚C, respectively.

## Tables and Figures:

**Table 1. Chemical composition (wt. %) of Cu-Al-Mn shape memory alloy used in the study**

| **Cu** | **Al** | **Mn** | **Fe** |
|---|---|---|---|
| Bal. | 9.77 | 13.17 | 0.12 |

**Table 2. Samples naming and anodizing parameters**

| Sample | Voltage (V) | T(˚C) |
|---|---|---|
| A0520 | 20 | 5 |
| A0530 | 30 | |
| A0540 | 40 | |
| A0550 | 50 | |
| A1020 | 20 | 10 |
| A1030 | 30 | |
| A1040 | 40 | |
| A1050 | 50 | |

**Table 3. Potentiodynamic tests results in 1M Nacl solution**

| Sample | Corrosion current density (μA.cm$^{-2}$) | Corrosion potential (E vs SCE) | **β**a (V/decade) | **β**c (V/decade) | Rp(ohm) | C.R. (mpy) ×10$^{-8}$ |
|---|---|---|---|---|---|---|
| A0520 | 1.31 | -0.43 | 0.0143 | 0.0326 | 4475 | 1.91 |
| A1050 | 1.58 | -0.48 | 0.0444 | 0.2445 | 10328 | 2.31 |
| Al coated | 2.13 | -0.46 | 0.0311 | 0.2350 | 5600 | 3.11 |
| Uncoated | 2.51 | -0.34 | 0.0388 | 0.0776 | 3295 | 3.67 |

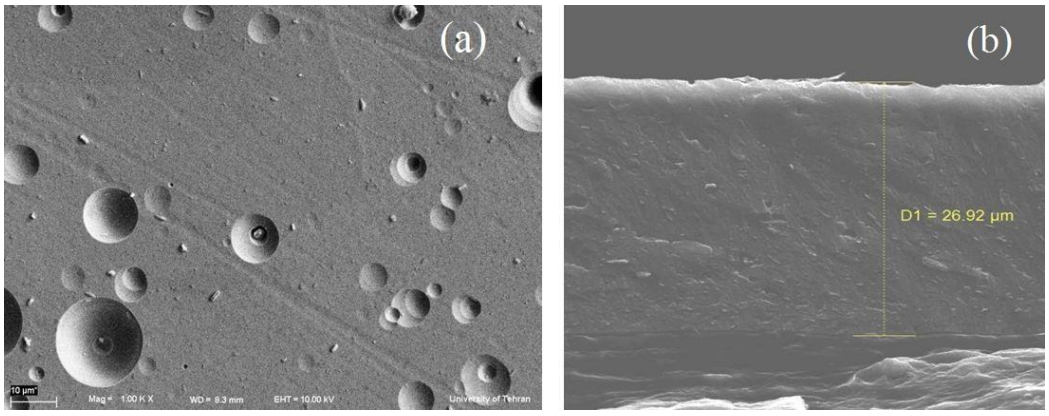


**Fig.1: The SEM micrograph of AlN coatings deposited onto the Cu-10Al-13Mn alloy substrates: (a): surface, (b): cross section**

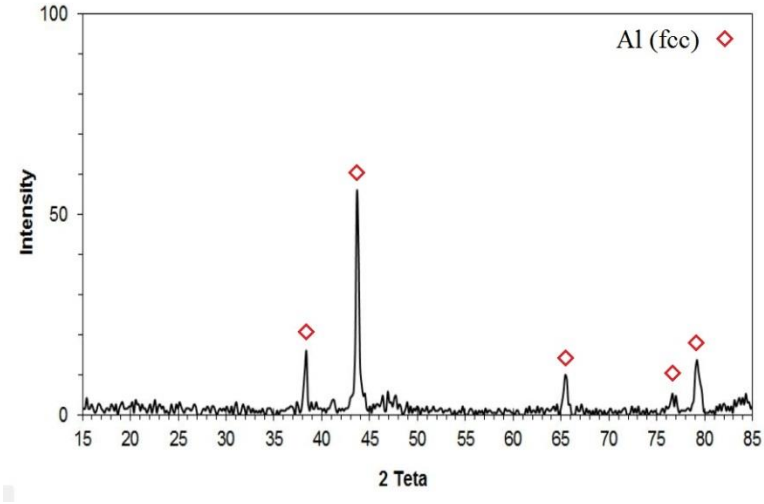


**Fig.2: XRD analysis of the Al coating on the Cu-10Al-13Mn alloy**

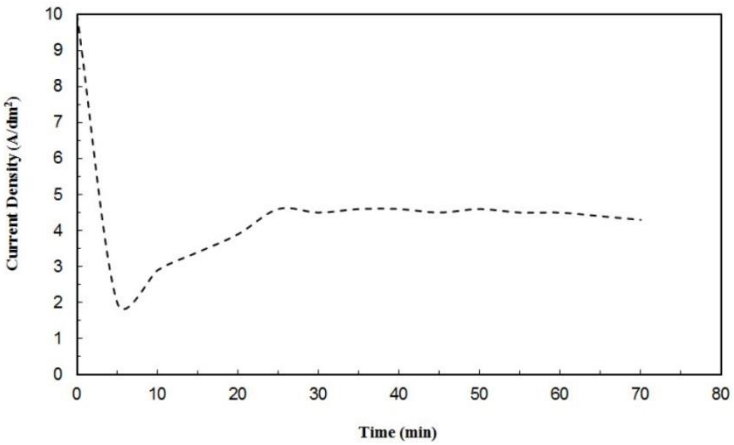


**Fig. 3: The current density by time during anodizing process**

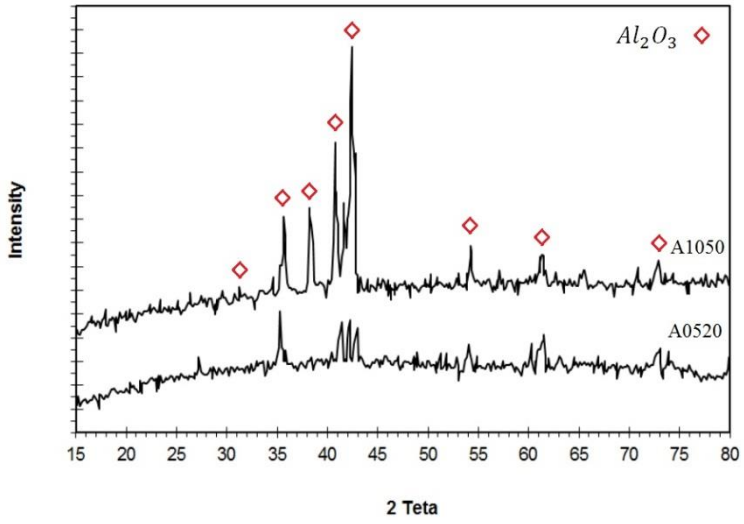


**Fig. 4: XRD analysis of the anodized Al coatings on the Cu-10Al-13Mn alloy**

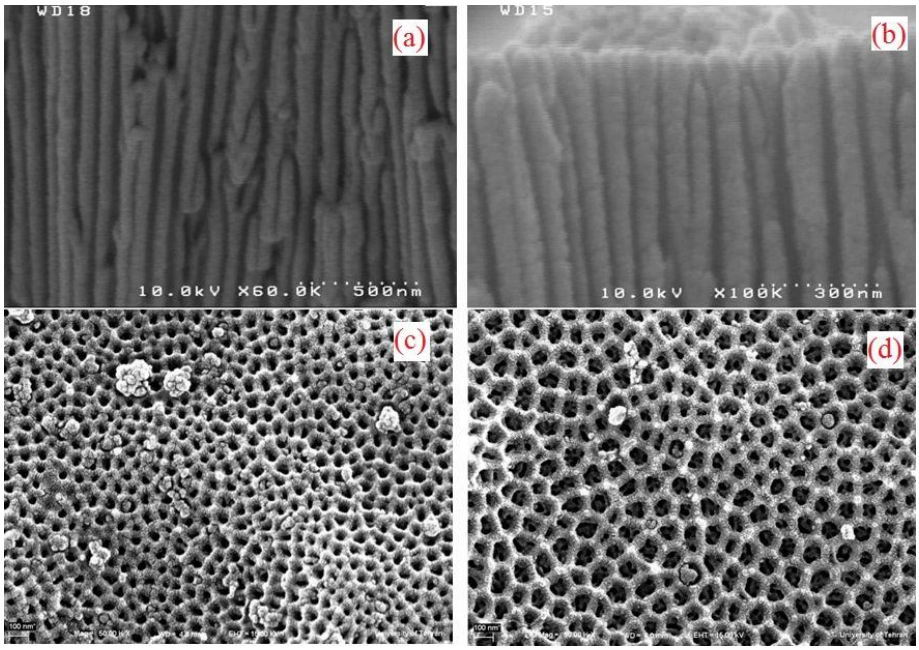


**Fig. 5: The SEM micrograph of anodized Al coatings deposited onto the Cu-10Al-13Mn alloy substrates: (a): cross section A0520, (b): cross section A1050, (c): surface A0520, (d): surface A1050**

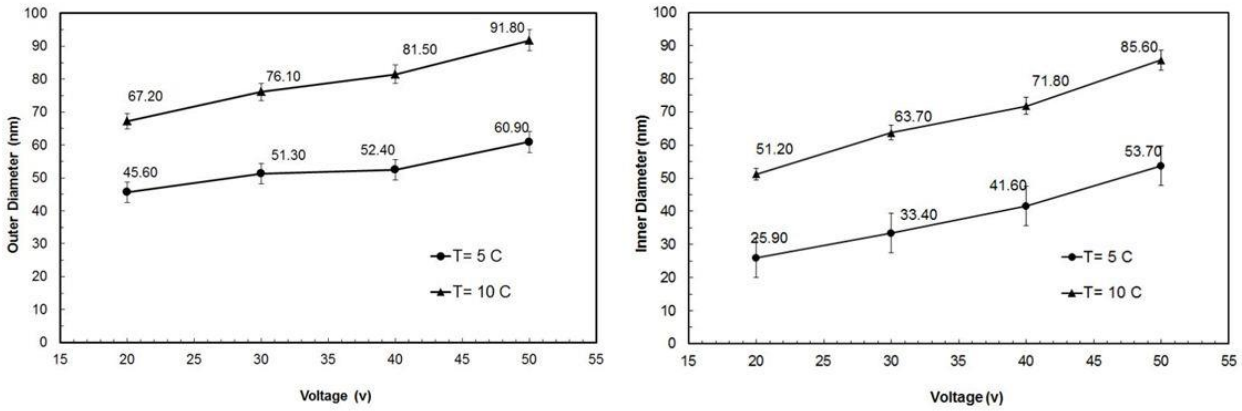


**Fig. 6: The Alumina nanotube dimension by voltage: (a): Inner diameters, (b): outer diameters**

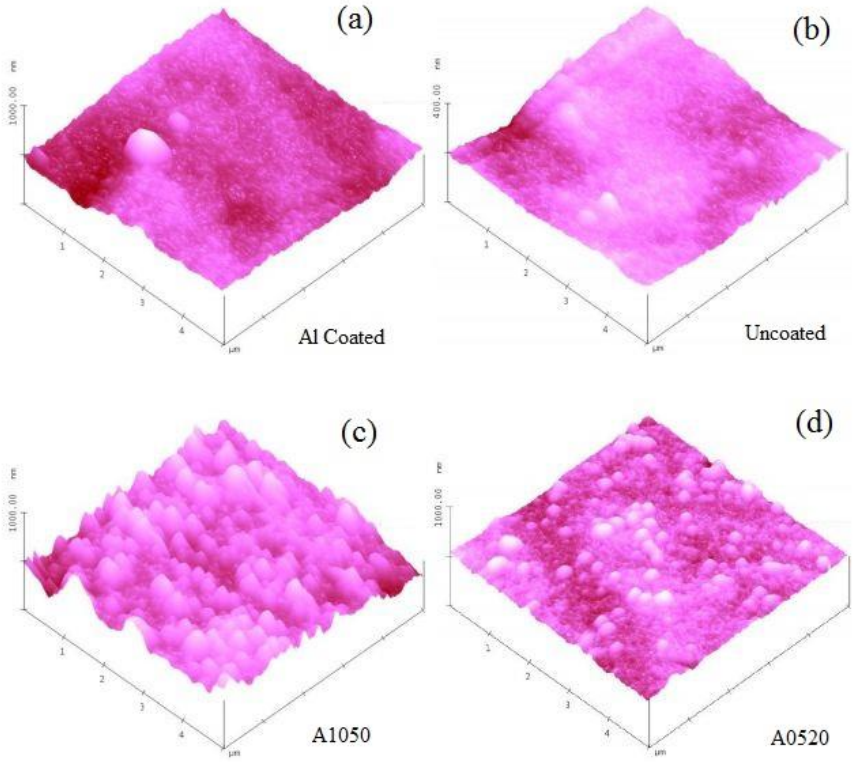


**Fig.7: Surface topography: (a): Al coated, (b): Uncoated, (c): A1050, (d): A0520**

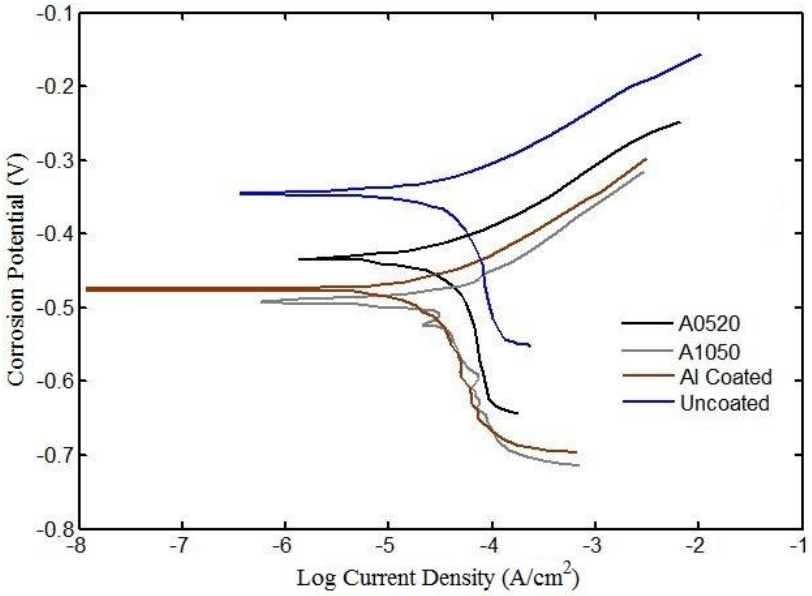


**Fig. 8 Potentiodynamic polarization curves of specimens: uncoated, Al coated, A1050, A0520**

## References:


[1] Otsuka K. and Wayman C. M.: Cambridge university press, 1999, 1-4.

[2] Sutou Y., Omori T., Wang J.J., and et al., *Materials Science and Engineering: A*, 2004,***378***(1),278.

[3] Zheng Y., Li C., Wan F. and Long Y., *Journal of alloys and compounds*, 2007,***441***(1),317.

[4] Zak G., Kneissl A.C., and Zatulskij G., *Scripta materialia*,1996,***34***(3),363.

[5] Blazquez M.L., Lopez Del Castillo C., and Gomez C., *Metallography*, 1989,***23***(2),119.

[6] del Castillo C.L., Mellor B.G., Blazquez M.L., and et al., *Scripta metallurgica*,1987,***21***(12),1711.

[7] Mallik U.S., and Sampath V., *Journal of Alloys and Compounds*, 2008,***459***(1),142.

[8] Benatti O.F., Miranda W.G. and Muench A,. *The Journal of prosthetic dentistry*, 2000,***84***(3),360.

[9] Tibballs, J.E. and Erimescu, R., *dental materials*, 2006,***22***(9),793.

[10] Gojić M., Vrsalović L., Kožuh S., and et al., *Journal of alloys and compounds*, 2011,***509***(41),9782.

[11] Sürry P. and Oswald H.R., *Corrosion Science*, 1972,***12***(1),77.

[12] Guosong W., Zeng X., and Yuan G., *Materials Letters*, 2008,***62***(28),4325.

[13] Dixit G., and Anthony K., U.S. Patent No. 6,355,558., 2002.

[14] Shakoori Oskooie M., Sadeghpour Motlagh M., and Aghajani H., *Surface and Coatings Technology*, 2016,***291***,356.

[15] Handbook, A. S. M. "Vol. 5." *Surface Engineering*, 1982,619.

[16] Ajeel S. A., Kasser N. W., and Abdul-Hussein B. A., *Modern Applied Science*, 2010,***4***(5),87.

[17] Buzzard R.W., *Journal of Research of The National Bureau of Standards*, 1937,***18***,251.

[18] In-Joon, S.O.N., Nakano H., Satoshi O.U.E., and et al., *Transactions of Nonferrous Metals Society of China*, 2009,***19***(4),904.

[19] Huang Y., Shih H., Huang H., and et al., *Corrosion Science*, 2008,***50***(12),3569.

[20] Zhang J.S., Zhao X.H., Zuo Y., and et al., *Surface and Coatings Technology*, 2008, ***202***(14),3149.

[21] Xingwen Y., and Cao C., *Thin Solid Films*, 2003,***423***(2),252.

[22] Zuo Y., Zhao P.H. and Zhao J.M., *Surface and Coatings Technology*, 2003,***166***(2),237.

[23] Chiu L.H., Chen C.C. and Yang C.F., *Surface and Coatings Technology*, 2005,***191***(2),181.

[24] Li X., Nie X., Wang L., and et al., *Surface and Coatings Technology*, 2005,***200***(5),1994.